International Journal of Nanomedicine

Dovepress
open access to scientific and medical research

Open Access Full Text Article

ORIGINAL RESEARCH

Engineering of Amphiphilic Erlotinib Analogue as Novel Nanomedicine for Non-Small Cell Lung Cancer Therapy

Mei Cong[1,*], Houjun Pang[1,2,*], Guangxing Xie[1], Feifei Li[3], Chunxiao Li[3], Hao Sun[3], Shaoyou Yang[1], Weidong Zhao[3]

[1]School of Pharmacy, Xinxiang Medical University, Xinxiang, People's Republic of China; [2]Department of Pharmacy, Dazhou Women and Children's Hospital, Dazhou, People's Republic of China; [3]Henan Key Laboratory of Immunology and Targeted Drugs, School of Laboratory Medicine, Xinxiang Medical University, Xinxiang, People's Republic of China

*These authors contributed equally to this work

Correspondence: Weidong Zhao, Henan Key Laboratory of Immunology and Targeted Drugs, School of Laboratory Medicine, Xinxiang Medical University, Xinxiang, 453003, People's Republic of China, Tel +86 0373 3029977, Fax +86 0373 3029977, Email 141051@xxmu.edu.cn

Purpose: Molecular targeted therapy is one of the most pivotal strategies in the treatment of non-small cell lung cancer, yet its curative effect is severely compromised by the poor aqueous solubility, low bioavailability and inadequate tumor accumulation of targeted agents. To enhance the efficacy of targeted agents, we demonstrate a novel self-assemble amphiphilic molecule based on erlotinib as an effective nanodrug for anti-cancer treatment.

Methods: An amphiphilic molecule composed of hydrophobic erlotinib and hydrophilic biotin block was synthesized and characterized by nuclear magnetic resonance (NMR) as well as high-resolution mass spectrometry (HRMS). Then, nanoassemblies of the amphiphilic molecules are formulated by using nanoprecipitation method. Subsequently, the size, morphology, cell uptake, the anticancer activity and in vivo distribution of the newly constructed erlotinib nanodrug were systematically assessed by some methods, including transmission electron microscopy (TEM), dynamic light-scattering (DLS), flow cytometry, in vivo imaging system etc.

Results: We developed a novel nanoformulation of erlotinib, which possesses a high drug loading of 45%. With the features of well-defined structure and small size, the obtained nanodrug could be effectively accumulated in tumor sites and rapidly internalized by cancer cells. Finally, the erlotinib-based nanoformulation showed considerably better anticancer activity compared to free erlotinib both in vitro and in vivo. Moreover, the nanodrug displayed great tolerability.

Conclusion: Combining the advantageous features of both nanotechnology and self-assemble, this novel erlotinib nanomedicine constitutes a promising therapeutic candidate for cancer treatment. This study also underlines the potential use of amphiphilic molecule for improving drug efficacy as well as reducing drug toxicity, which could become a general strategy for the preparation of nanodrugs of active agents.

Keywords: erlotinib, amphiphilic molecule, self-assembling, drug self-delivery system, non-small cell lung cancer

Introduction

Lung cancer is the most common cause of cancer mortality worldwide, of which non-small-cell lung cancer (NSCLC) is the main subtype.[1,2] Despite the use of molecularly targeted agents, including osimertinib, afatinib, dacomitinib, gefitinib and erlotinib, has achieved important advancements in the treatment of NSCLC, the 5-year survival rate remains low.[2,3] Erlotinib (Eb) is used as the clinical drug either alone or in combination, to treat NSCLC and pancreatic cancers, via inhibiting the phosphorylation of epidermal growth factor receptor, leading to the suppression of downstream signaling pathways, and consequent inhibition of cell proliferation, angiogenesis and metastases.[4–6] However, its clinical anticancer activity is restricted by poor aqueous solubility, less drug accumulation and variable bioavailability.

Received: 22 August 2023
Accepted: 31 October 2023
Published: 7 November 2023

Erlotinib belongs to class II in the Biopharmaceutical Classification System (BCS) due to low water solubility and high permeability.[7] The intrinsic aqueous solubility of Eb is less than 5 μg/mL at neutral pH and with increased solubility at pH < 5 (the maximum solubility ~0.4 mg/mL at pH 2).[7–10] When Eb is orally administered, it is quickly absorbed by the gastrointestinal tract.[8,11] However, its poor intrinsic water solubility limits the dissolution of the agent in the gastrointestinal fluid (aqueous) that can restrict its absorption,[12] resulting in large fluctuation in its bioavailability and substantial interpatient pharmacokinetic variability, which seriously hampers the therapeutic efficacy and clinical applications.[8,10–12] Furthermore, it has been reported that patients receiving this agent suffered from dose-related side effects, such as skin rash, gastrointestinal disorders, Stevens-Johnson syndrome, kidney and liver damages.[13–17] Among of these adverse events, skin rash and gastrointestinal disorders are frequently observed in up to 76% and 55% of the patients, respectively, leading to the discontinuation of therapy.[17] Therefore, there is a dire need to establish an efficient strategy to address these problems.

Recent studies have shown that nanotechnology-based drug delivery system could overcome the limitations experienced, and thus effectively enhancing the Eb-based therapy.[18–21] Particularly, nanocarrier-based drug delivery system (DDS) is a promising approach, which can obviously improve the drug efficacy by encapsulating the active pharmaceutical ingredients into nanoparticles or coupling onto the surface of the nanocarriers.[22,23] By taking advantage of nanocarriers, the traditional nanocarrier-based drug delivery systems can not only improve drug bioavailability but also reduce the side effects of drugs, which can significantly enhance drug targeting to tumor tissue.[18,23] To date, different nanocarrier-based nanosystems have been established for improving the therapeutic efficiency of Eb, with liposome and polymer carriers being the most widely used.[18,21,24–26] Nonetheless, most of these nanocarrier-based DDSs are hard to translate from bench to bedside due to the complicated composition and poor stability which hamper the scalable production.[27–29] In addition, as additional carriers account for the major part of the mass of both liposome- and polymer-based drug delivery systems, the drug loading is rather low, which further limits their therapeutic efficacy.[20,30–32] Thus, the development of alternative drug delivery strategies without using any additional carriers is extremely desirable.

Amphiphilic molecules that can spontaneously assemble into well-defined nanostructures without the aid of additional carriers represent a potential strategy for constructing nanoformation.[33,34] This strategy also named drug self-delivery systems (DSDSs),[34] which has attracted great attention thanks to some remarkable properties: (I) Comparing with free drugs, the amphiphilic molecules have better delivery efficiency and higher tumor accumulation via the enhanced permeability and retention (EPR) effect;[35] (II) The active pharmaceutical ingredient itself, in addition to its therapeutic effect, also performs a function as carrier within the amphiphilic conjugate thus effectively reducing the amount of carrier required and avoiding the potential toxicity associated with the inert carriers; (III) The simple and stable structures are benefit for large scalable production.

Here, we report a novel drug self-delivery system of target agent Eb, which exhibited potent anticancer activity against NSCLC. Specially, we designed and synthesized an amphiphilic molecule (Figure 1), in which the hydrophobic

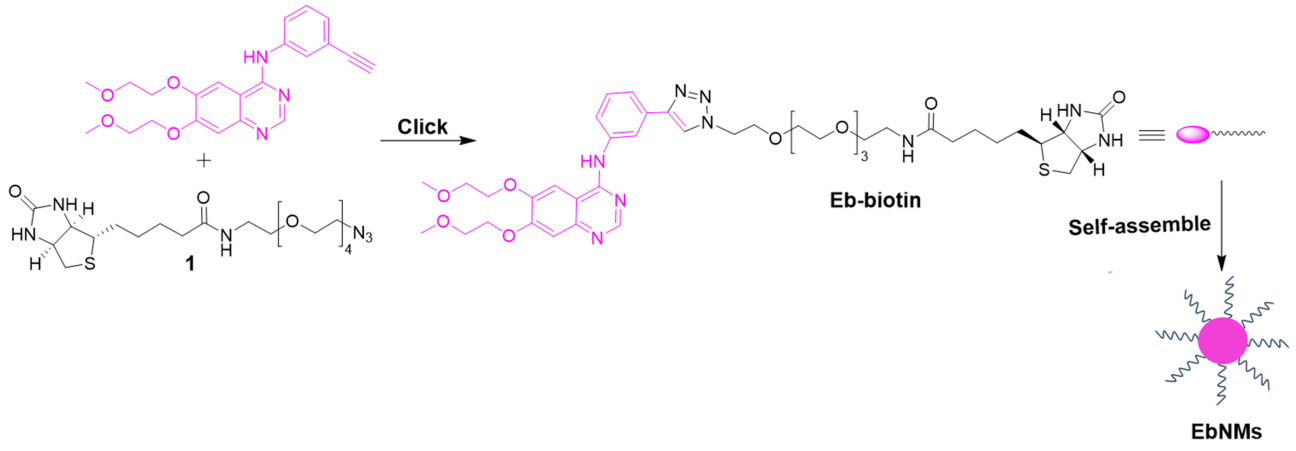

Figure 1 Schematic route of Eb-Bio conjugate and construction of self-assemble nanodrug (EbNMs) for improving the anticancer efficacy of Eb-based chemotherapy.

drug Eb and the hydrophilic biotin analogue were linked to each other by click reaction. Biotin receptors are over-expressed at the surface of many cancer cells, which have been used for constructing active tumor targeting therapies.[36,37] Therefore, biotin was introduced into the amphiphilic prodrug to facilitate its accumulation in tumor tissue via the receptor-mediated internalization. By virtue of its amphiphilicity, the Eb-biotin (Eb-Bio) conjugate could self-assemble into nanomicelles in aqueous solution, which selectively delivered Eb to tumor tissue and enhanced the cell uptake. Consequently, more significant anticancer activity was observed compared to free Eb, both in vitro and in vivo.

Materials and Methods

General Materials

The chemical reagents used were purchased from Aldrich or Aladdin or Macklin or TCI, which were used without further purification. Analytical thin-layer chromatography (TLC) was performed using silica gel 60 F254 plates 0.2 mm thick with UV light (254 and 364 nm) as revelator. Chromatography was prepared on silica gel (Merck 200–300 mesh).^{1}H NMR spectra were recorded at 400 MHz and ^{13}C NMR spectra recorded at 100 MHz, on VARIAN INOVA-400M. HRMS spectra were obtained on Bruker 7-Tesla FT-ICR MS equipped with an electrospray source. The A549 cell line was purchased from National Infrastructure of Cell Line Resource. The cells were cultured with Dulbecco's Modified Eagle Medium (DMEM) with 10% fetal bovine serum (FBS) and maintained in a 37°C incubator with 5% CO_2 humidified atmosphere.

Synthesis, Preparation and Characterization of EbNMs Nanomicelles

General Procedure for Synthesis of Eb-Bio Conjugate

To a Scheck tube was added Eb (28 mg) and tris(3-hydroxypropyltriazolylmethyl)amine (6.2 mg). The vessel was sealed and purged with argon for 5 min. The solution of Biotin-PEG_4-azide (34 mg) in tetrahydrofuran (THF, 3.2 mL), $CuSO_4 \cdot 5H_2O$ (4.0 mg) and sodium ascorbate (6.2 mg) in H_2O (0.80 mL) were then added into the tube. The resulting reaction mixture was stirred at room temperature (r.t.) until the reaction was completed indicated by TLC. The THF was evaporated from the reaction mixture under reduced pressure, and the yielded residue was dissolved in dichloromethane (DCM), washed with distilled water, and dried over $MgSO_4$. DCM was then evaporated to yield a crude product, which was further purified by column chromatography on silica gel using DCM/CH_3OH as eluent, yielding Eb-Bio conjugate (34 mg, 55%) as a white solid. ^{1}H NMR (400 MHz, CD_3OD) δ 8.40 (t, J = 6.2 Hz, 2H), 8.25 (s, 1H), 7.85 (s, 1H), 7.73 (s, 1H), 7.62 (d, J = 7.7 Hz, 1H), 7.47 (d, J = 7.9 Hz, 1H), 7.18 (s, 1H), 5.38–5.25 (m, 1H), 4.65 (t, J = 4.8 Hz, 2H), 4.50–4.11 (m, 6H), 3.97–3.81 (m, 5H), 3.72–3.37 (m, 18H), 3.33 (s, 3H), 3.15–3.05 (m, 1H), 2.84 (s, 1H), 2.64 (d, J = 12.7 Hz, 1H), 2.19–1.97 (m, 4H), 1.59–1.54 (m, 6H), 0.88 (t, J = 6.5 Hz, 4H). ^{13}C NMR (101 MHz, CD_3OD) δ 174.6, 164.7, 157.2, 154.7, 152.7, 149.1, 147.0, 146.2, 139.7, 131.0, 129.1, 122.3, 122.0, 121.1, 119.6, 109.3, 106.8, 102.8, 70.5, 70.1, 69.7, 69.0, 68.7, 68.3, 67.5, 61.9, 60.2, 58.1, 55.6, 50.2, 39.7, 38.9, 35.3, 29.5, 28.3, 28.1, 25.4, 25.1. HRMS: calcd. for $C_{42}H_{59}N_9O_{10}S$, $[M+H]^+$ 882.4184, found 882.4173.

Critical Micelle Concentration (CMC) Measure

The critical micelle concentration (CMC) of Eb-Bio conjugate was assessed using pyrene as the fluorescent probe.[38] A serial Eb-Bio conjugate solution ranging from 3.13×10^{-6} to 1.0×10^{-4} mol/L was prepared in MilliQ water and diluted in MilliQ water to get desired concentration in 1.0 mL. Then, 1 μL of pyrene solution (0.6 mM) was added and subsequently sonicated for 30 min. The so-obtained solution was kept for 2 h at room temperature to finalize the micelle formation. Then, the fluorescent spectra were measured at the excitation wavelength of 335 nm on a fluorescence spectrophotometer (RF-5301PC; Shimadzu). The fluorescent intensity ratio of I_{373}/I_{384} was analyzed as a function of logarithm Eb-Bio conjugate concentration. A fit linear analysis to the fluorescence data was applied.

Nanoparticle Preparation

Nanoparticle was prepared by the nanoprecipitation,[38–40] the commonly used strategy for self-assemble nanodrug preparation. Method 1: Eb-Bio conjugate 50 mM (concentration of Eb) in dimethylsulfoxide (DMSO) was prepared.

The solution (2.0 μL) was then added slowly under vigorous stirring to 2.0 mL of phosphate-buffered saline (PBS) at pH 7.4 in a centrifuge tube.

Method 2: Eb-Bio conjugate in ethanol (10 mg/mL, concentration of Eb) with 2.5% v/v Tween 80 was prepared. The obtained organic solution was then added dropwise under vigorous stirring to PBS solution at pH 7.4 in a centrifuge tube. Formation of the nanoparticles occurred spontaneously and stirring was continued for several minutes. The suspension was then evaporated using a Rotavapor to remove the organic solvents.

For the internalization experiments, Doxorubicin (DOX) was dissolved in DMSO and mixed with Eb-Bio conjugate, then the resulted organic solution was added into PBS. Subsequently, the obtained solution was filtered to remove the unencapsulated compound. For the in vivo imaging, 1 1'-dioctadecyl-3,3,3',3'-tetraMethylindotricarbocyanine iodide (DiR) was used for the preparation of fluorescence-labelled EbNMs/DiR nanosystem by the following procedure: DiR was dissolved in DMSO and mixed with Eb-Bio conjugate and 40% v/v PEG300, then the resulted organic solution was added into PBS at pH 7.4 in a centrifuge tube. Finally, the obtained solution was filtered to remove the unencapsulated compound.

Micelle Morphology Characterization

The morphology of nanomicelles was determined using transmission electron microscope (TEM). Briefly, the solution of EbNMs was dropped onto the copper grids and air-dried at 42°C. The grids were stained with 1.0% (wt/vol) uranyl acetate solution for 30s before taking images. Then, imaging was performed using a JEM-1200EX analytical electron microscope.

Micelle Size Characterization

Hydrodynamic sizes of the nanomicelles were measured in aqueous solution by dynamic light scattering (DLS) (Zetasizer Nano-ZS90, Malvern).

In vitro Antiproliferation Activity Assay

The antiproliferation activity of free Eb, biotin, and EbNMs against human lung cancer cells was evaluated using Cell Counting Kit-8 (CCK8) assays. A549 cells were seeded in a 96-well plate at an initial density around 4, 000 cells per well, and allowed to adhere at 37°C for 24 h. Then, the culture medium was removed and replaced with fresh media alone as control or containing different drug formulation and further incubated for 72 h. Subsequently, the number of viable cells remained was determined by CCK8 assay. All experiments were done in triplicate and repeated three independent times.

Internalization of Free DOX and EbNMs/DOX Nanomicelles

Internalization of free DOX and EbNMs/DOX nanomicelles in A549 cells was examined using flow cytometry. A549 cells were seeded into 6-well plates at an initial density around 3×10^5 per well and incubated at 37°C overnight. Subsequently, the medium was then removed and replaced with different formations of DOX for 5, 20, 60, 120, 180 and 240 min at 37 ^{o}C. Finally, the cells were harvested and washed with 1× PBS solution three times and then analyzed on the flow cytometer (FACS Calibur, BD). Each assay was performed in triplicate.

In vivo Anticancer Activity Assay

The in vivo behavior of free Eb and EbNMs was investigated in a lung cancer A549 tumor-bearing mouse model. All animal experimental protocols were performed according to guidelines provided by the Institutional Animal Care and Use Committee (IACUC) of the Xinxiang Medical University and approved by the Ethics Committee of Xinxiang Medical University (2019/11/20, XYLL-2019S017). Four-weeks-old female Balb/c nude mice were purchased from Vital River Laboratories (Beijing, China) and bred in the authorized SPF (specific pathogen free) animal facility at Xinxiang Medical University. To establish xenograft mice model, lung cancer cell A549 (1×10^6) into in 0.1 mL of cold PBS were injected subcutaneously into the right axilla of nude mice. When the tumor size reached about 50–100 mm^3 by average, the xenograft mice were randomly divided into three groups (day 0), the control group, the Eb group, the

EbNMs group. Mice were intravenously injected with corresponding compounds at an Eb dose of 2.5 mg/kg body weight via the tail vein. The mice were treated every three days for four times. The tumor progression in the mice was measured twice a week by Vernier calipers, and the tumor volume was calculated as described previously.[21] The mice were weighted every three days. On day 15, the experiment was halted and animals in each group were sacrificed. The kidney, liver and tumor tissue were harvested and fixed in 4.0% paraformaldehyde solution for histopathological analysis.

Histopathological Analysis

Histopathological analysis was performed by a Hematoxylin and Eosin (HE) staining kit purchased from Servicebio (G1003) according to the manufacturer's protocol with slight change. Tissues were fixed in 4.0% paraformaldehyde at room temperature for at least 24 h. Then, paraffin-embedded specimens were cut into 5.0 μm sections, which were mounted on glass slides. Images were taken under a light microscope (Nikon eclipse E100). Paraffin sections of different organs were deparaffinized twice by immersion in xylene for 20 min each time and rehydrated in a series of gradual alcohols (absolute ethanol I for 5 min, absolute ethanol II for 5 min, 75% alcohol for 2 min). Followed by rinsing them in distilled water and staining with hematoxylin solution for 3–5 min. Then, the slices were washed in running tap water. Then, the sections were differentiated with Hematoxylin Differentiation solution and terminated by rinsing with in tap water. Then, the slices were treated with Hematoxylin Scott Tap Bluing, and washed by tap water. The slices were treated with 85% alcohol for 5 min and 95% alcohol for 5 min, and further stained with Eosin dye for 5 min. The slices were dehydrated 3 times in absolute ethanol for 5 min each time. Afterwards, the obtained slices were cleared in xylene twice for 5 min each time and sealed by natural gum.

In vivo Biodistribution

To determine the in vivo biodistribution of nanodrugs, A549 tumor-bearing female Balb/c nude mice were injected intravenous with free DiR and EbNMs/DiR nanomicelles at a dose of 60 μg/Kg of DiR via the tail vein. The distribution and tumor accumulation of free DiR and EbNMs/DiR nanomicelles were recorded at 4 h and 24 h post administration, using an in vivo imaging system (PerkinElmer IVIS Lumina III). Then, mice were sacrificed and the organs including heart, liver, spleen, lung, and kidney as well as tumor were excised. The fluorescence images of major organs and tumor tissues were obtained by using PerkinElmer IVIS Lumina III imaging system.

Statistics

Statistical analysis was evaluated with GraphPad Prism v6 software. All the data were expressed as the means ± standard error of the mean (SEM). Unpaired Student's *t*-test (two-tailed) was applied to determine differences between the two means. Two-way ANOVA followed by a Tukey's multiple comparisons test was used for multiple comparison in the groups. And $P < 0.05$ was considered statistically significant.

Results and Discussion

Synthesis and Characterization of Eb–Bio Conjugate

To improve the therapeutic efficacy of erlotinib, a novel nanodrug based on the linkage of erlotinib and biotin was constructed and termed Eb-Bio conjugate. The Eb-Bio conjugate was synthesized via click chemistry using the azido-carrying biotin analogue (biotin-PEG_4-azide) and erlotinib (Figure 1). The reaction proceeded very well, and the conjugate was obtained in pure state, as confirmed by NMR spectroscopy and high-resolution mass spectroscopy (Figures S1–S3 in Supporting information). Due to the covalent conjugation, erlotinib–biotin conjugate has high and stable drug payload up to 45 wt% calculated from its molecular structure and chemical composition.

Eb–Bio Conjugate Efficiently Improved the Aqueous Solubility of Erlotinib via Self-Assemble into Nanomicelles with Small Size

It has been reported that the poor water solubility of Eb hinders its bioavailability and absorption, which seriously limits the therapeutic efficacy and clinical applications.[8,10–12] Several strategies regarding to overcome these limitations have been employed in the literature. Among them, nanonization is expected to increase the dissolution rates and bioavailability of drugs with poorly water solubility by increasing the surface area.[41,42] Therefore, the performance of self-assembling into nanoparticles of Eb–Bio conjugate was determined. The self-assembly of Eb–Bio conjugate was observed by measuring its critical micelle concentration (CMC) using fluorescence spectroscopy with pyrene as fluorescent probe (Figure 2A). The self-assembling ability of Eb–Bio conjugate was proved with a CMC value of 13 μmol/L. It formed small spherical nanomicelles (referred to as EbNMs) of 9.5 ± 0.4 nm in aqueous, with a polydispersity index of 0.06 ± 0.03 as revealed by results obtained from dynamic light scattering analysis (Figure 2B). This was further confirmed by transmission electron microscopy, which obviously demonstrated the formation of small size particles with dimensions in the range of nanomicelles (Figure 2C). Moreover, the zeta potential of EbNMs, observed to be around −20 mV (Figure 2D), could generate electrostatic repulsion and prevent aggregation of particles, making EbNMs colloidally stable. Notably, the nanoparticles with negatively charged would be expected to display a repulsive interaction with the cell membrane and serum proteins that often take negatively charge, thereby being less toxic. All these results indicate that EbNMs are able to spontaneously self-assemble into stable small size nanomicelles, effectively improving the dissolution of Eb in aqueous solutions.

EbNMs Enhanced Antiproliferation Efficiency of Eb on Lung Cancer Cells Through Rapid and Effective Cellular Uptake

Motivated by the self-assemble ability and subsequently the improved dissolution of Eb-Bio conjugate, we further assessed the antiproliferative activity of EbNMs by using CCK8 assays in human A549 cell line. Both free Eb and EbNMs displayed concentration-dependent ability to inhibit the cancer cell proliferation (Figure 3A). Biotin had no

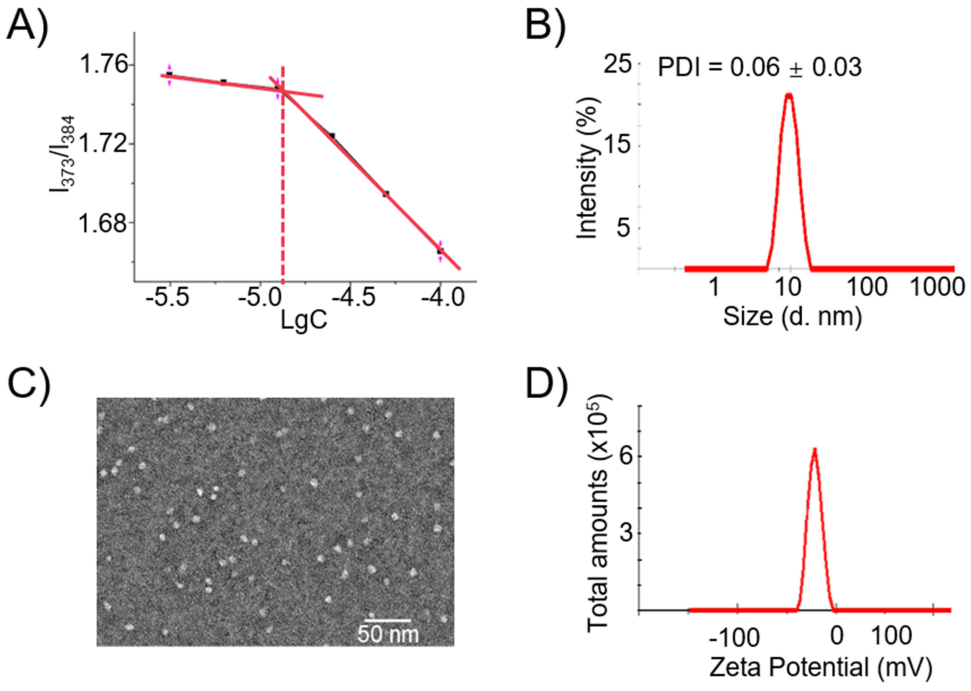

Figure 2 Self-assembling of the amphiphilic Eb-Bio conjugate into nanomicelles (EbNMs). (**A**) The critical micelle concentration of Eb-Bio conjugate determined using fluorescent assay with pyrene as the fluorescent probe; (**B**) dynamic light scattering (DLS) analysis; (**C**) transmission electron microscopic (TEM) imaging; (**D**) zeta potential measurement of the EbNMs.

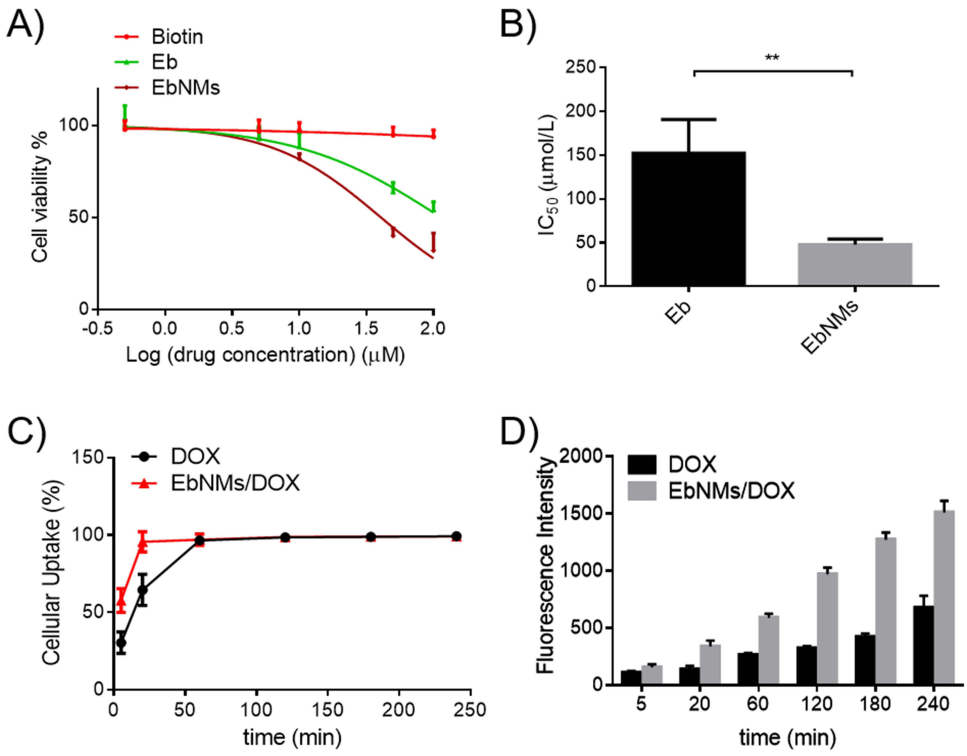

Figure 3 Nano carrier free nanodrug EbNMs shows enhanced antiproliferation efficiency via rapid and effective cellular uptake. (**A**) The antiproliferative activity of free Eb, biotin and EbNMs on lung cancer A549 cells was measured using an CCK8 assay. (**B**) IC50 values for EbNMs on A549 cells in comparison with that of Eb. (**C**) Kinetics of cellular uptake (%) of free drug and nanodrug in A549 cells were analyzed by flow cytometry. (**D**) Mean fluorescence intensity of DOX in A549 cells treated with free Dox and EbNMs/Dox as function of incubation time. The experiment was repeated three times independently. The data are presented as the mean ± SEM. **p < 0.01.

impact on cell viability on the tested cells. Compared with free Eb, EbNMs exhibited higher antiproliferative activity on A549 cells. The half-maximal inhibitory concentration (IC_{50}) values for EbNMs and Eb were observed at 47.8±3.7 and 152.1±22.3 μmol/L ($p < 0.0099$), respectively (Figure 3B).

An augmented cellular uptake of nanomicelles may contribute to the enhanced antiproliferation activity of EbNMs. To test this possibility, a lipophilic drug DOX that has intrinsic fluorescence properties was loaded into EbNMs to forming a fluorescently labeled nanosystem. Then, the DOX-loaded nanomicelles (named EbNMs/DOX) were incubated with A549 cells. The cellular uptake of EbNMs/DOX was observed by using flow cytometry. As showed in Figure 3C, the cellular uptake of EbNMs/DOX was visibly rapid and efficient (Figure 3C and D) compared to that of free DOX. After 2 h treatment, the mean fluorescence intensity detected in EbNMs/ DOX treated cells was about 3 times higher than that of DOX treated cells (Figure 3D). These results suggest that the intracellular drug concentration was higher in cells treated with the EbNMs/ DOX than in cells treated with the free DOX, demonstrating convincingly that the enhanced antiproliferative effects of EbNMs might be attribute to the rapidly cellular uptake of the nanodrugs.

Superior Antitumor Activity and Enhanced Safety of EbNMs

We next investigated whether EbNMs displayed significant anticancer efficacy in a xenograft mouse model of lung cancer. A549 cells were injected into Balb/c nude mice to establish the mouse model. After the tumor reached the volume of 50–100 mm^3, the tumor-bearing mice were divided randomly and treated with either EbNMs (2.5 mg/kg of Eb equivalents) or free Eb (2.5 mg/kg) by intravenous injection every three days for up to 15 days. The dose of Eb selected in the experiment was based on our in vitro evaluation data and numerous reported studies with a view to assessing the efficacy and the safety of EbNMs. The tumor size and mice weight were measured every three days. As illustrated in Figure 4A, the mice treated with solvent vehicle, Eb and EbNMs, exhibited 4.16-, 2.69-, and 1.46-fold increases in A549 tumor volume at day 15, respectively. Clearly, the EbNMs nanodrug displayed great ability to suppress tumor growth compared with the other groups (Figure S4). This trend was further confirmed by terminal deoxynucleotidyl transferase

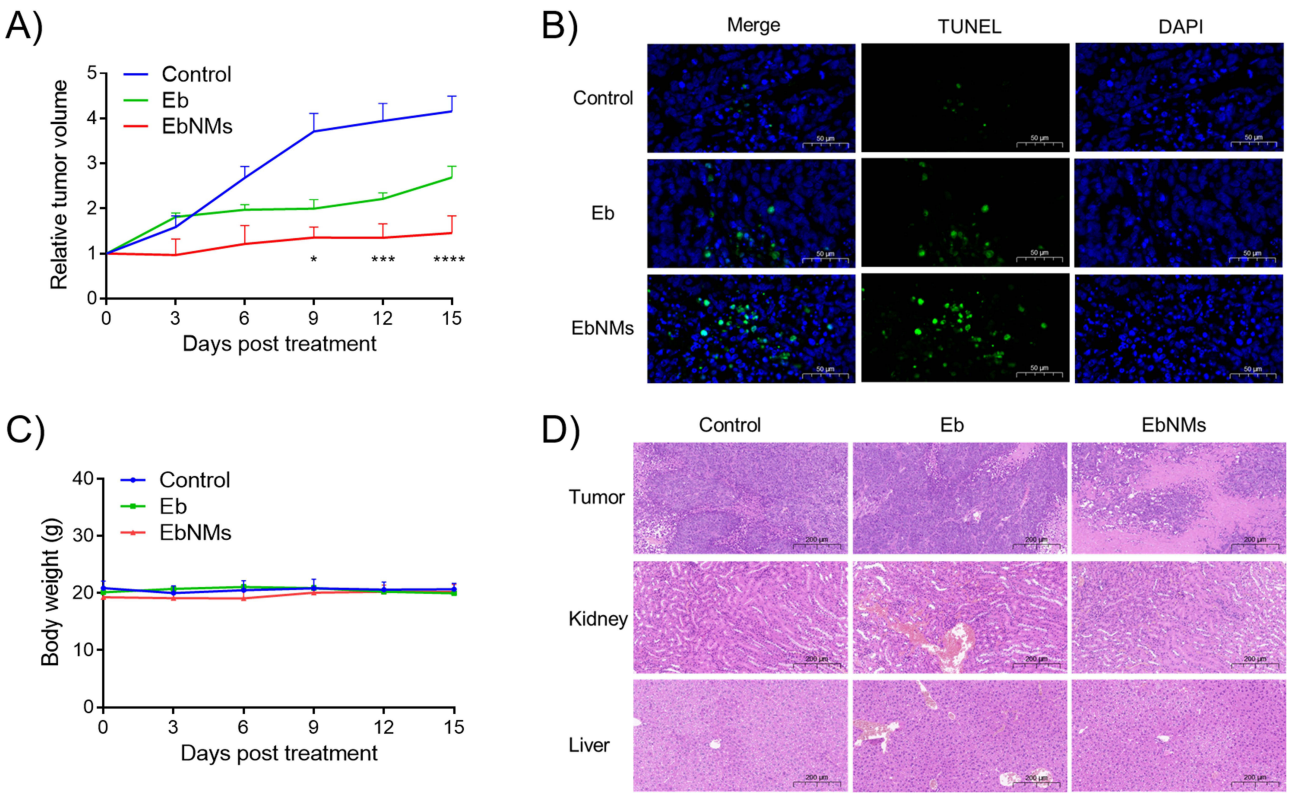

Figure 4 EbNMs significantly enhanced anticancer activity and reduced toxicity in tumor-xenograft mice. The mice were treated with free Eb and EbNMs at Eb dose of 2.5 mg/kg via i.v. administration (every 3 days, n= 3–4). (**A**) Effective antitumor activity of EbNMs in lung cancer A549 xenograft nude mice. (**B**) Terminal deoxynucleotidyl transferase dUTP nick-end labeling (TUNEL) staining of A549 tumor tissues after different treatments. (**C**) The mice body weight was recorded throughout the whole treatment period. (**D**) Histological analysis of tumor, liver and kidney. The data are presented as the mean ± SEM (n=3). *p < 0.05, ***p < 0.001, ****p < 0.0001.

dUTP nick-end labelling (TUNEL) staining, which demonstrated significantly increased apoptosis following EbNMs treatment (Figure 4B). All these results showed that treatment with EbNMs demonstrated more effective antitumor activity than free Eb.

During the course of the experiment, the body weight of mice was also recorded every 3 days. As presented in Figure 4C, no noticeable body weight alteration was observed in all groups, indicating good biocompatibility of the EbNMs nanodrugs. To further evaluate the associated toxicity in the different treatment groups, we performed histological studies by the hematoxylin and eosin (H&E) staining. The obvious tissue damages were detected in both liver and kidney in the free Eb treated group (Figure 4D), suggesting possible hepatotoxicity and nephrotoxicity associated with Eb, which was consistent with previous reports.[43] In contrast, there was no visible tissue damage in either kidney or liver in EbNMs treated group as compared with those in the control group. These results underline the enhanced safety of EbNMs compared with free Eb. Additionally, H&E staining showed that the nuclear fragmentation and shrinkage in tumor cells from EbNMs treated mice was more obviously than that of Eb-treated group (Figure 4D), further suggesting that EbNMs exerting efficient anticancer efficacy.

To understand the mechanism by which EbNMs augments the anticancer activities and enhanced safety, we investigated the distribution of the nanodrug and free drug in mice by using an in vivo imaging system. A near-infrared fluorescent dye DiR labeled EbNMs nanosystem (EbNMs/DiR) was generated and injected into the tumor-bearing A549 mice via the tail vein. The fluorescence signals in the mice were measured by a live imaging system. As shown in Figure 5A, the fluorescence signal of free DiR could not be detected at the tumor site after 24 h post-injection. In contrast, greatly strong fluorescence signals at the tumor site were detected in the EbNMs/DiR group (Figure 5A). This result suggested that the self-delivery nanodrug is more selectively enriched at tumor sites compared with free Eb, possibly thanks to the synergic effect of the active targeting of biotin and the EPR effect.

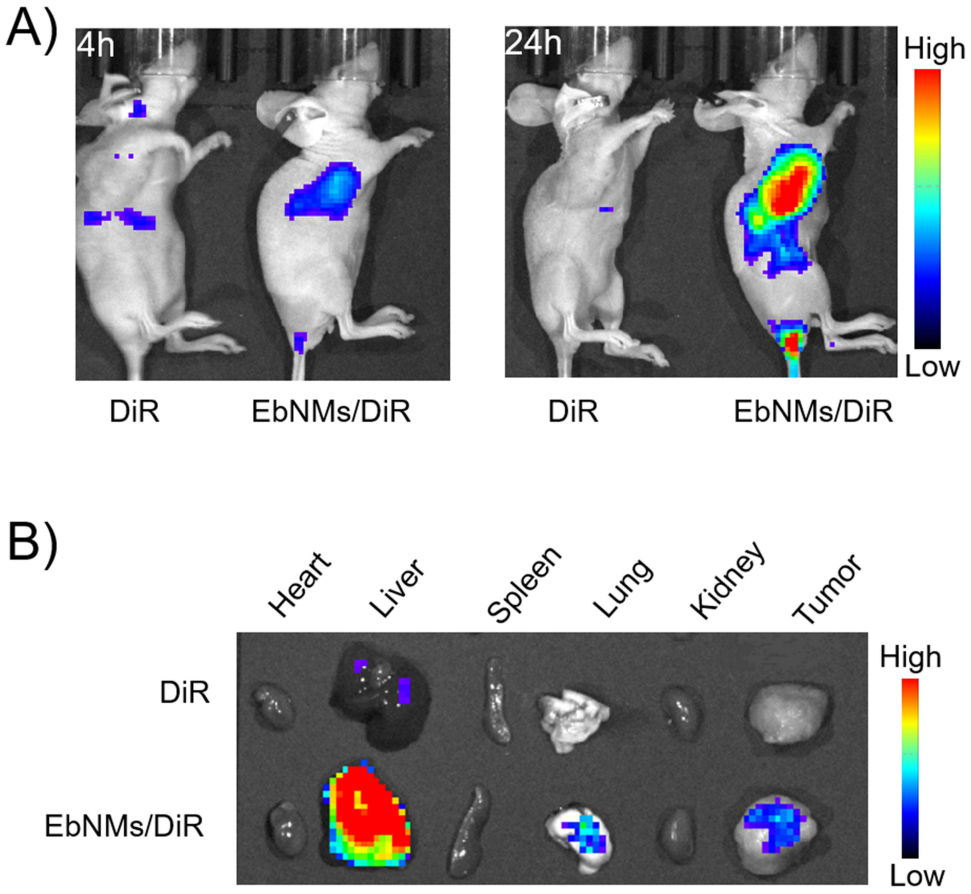

Figure 5 Biodistribution of the nanodrug EbNMs in mice by using in vivo images of mice with A549 xenograft tumors. (**A**) 4 h and 24 h after treatment with free DiR or EbNMs /DiR. (**B**) The images of ex vivo main organs and tumor after 24 h treatment.

Meanwhile, the biodistribution of different formulations at the major organs was also observed ex vivo by live imaging after the sacrifice of mice at 24 h post-injection. As illustrated in Figure 5B, no fluorescence signal was detected at tumor in the free DiR treated group. Whereas, EbNMs/DiR group clearly showed substantial drug accumulation at tumor and liver tissues, which was consistent with our experimental results on animal imaging. It is worth noting that the nanodrug exhibited the highest accumulation at livers compared with at other organs, suggesting this carrier-free Eb nanosystem could be easily excreted through liver, enabling it to be a desired drug delivery system. All these results demonstrate that EbNMs are capable of inducing the drug accumulation at tumor site, ultimately effectively enhancing anti-tumor activity and a good safety profile.

Conclusion

Non-small cell lung cancer is one of the most lethal malignancies that is usually detected at an advanced stage. Due to the limited efficiency of most current treatment regimens, together with the severe side effects, more effective agents are urgently needed. In this work, we have developed a novel self-assemble nanodrug of Eb, which is particularly promising because of its simple composition, small size and high drug loading. This structurally well-defined nanodrug significantly enhanced antitumor efficacy as displayed both in vitro and in vivo, thanks to the effective cellular internalization and selective accumulation at tumor site. Collectively, these results demonstrate that this novel nanodrug system constitutes a potential therapeutic candidate for NSCLC translational investigations. This study has also demonstrated the potential use of amphiphilic self-assemble prodrug for improving drug efficacy whereas enhanced safety.

Ethics Statement

The animal study was reviewed and approved by the ethics committee of Xinxiang Medical University.

Acknowledgments

This work was financed by grants from the National Natural Science Foundation of China (Nos. 81903567 and 31600109), the Innovation and Entrepreneurship Training Program for College Students in Henan Province (No. 202210472041), the PhD startup fund of Xinxiang Medical University (Nos. 505158 and 505097). We thank Jixia Zhang and Tangqiang Sun from Xinxiang Medical University for their help in the NMR experiments. We thank Zeqing Wu and Baoheng Lan from Xinxiang Medical University for their kind help in the biodistribution experiments.

Disclosure

The authors report no conflicts of interest in this work.

References

1. Siegel RL, Miller KD, Fuchs HE, et al. Cancer statistics, 2021. *Ca Cancer J Clin*. 2021;71(1):7–33. doi:10.3322/caac.21654
2. Thai AA, Solomon BJ, Sequist LV, et al. Lung cancer. *Lancet*. 2021;398(10299):535–554. doi:10.1016/S0140-6736(21)00312-3
3. Herbst RS, Morgensztern D, Boshoff C. The biology and management of non-small cell lung cancer. *Nature*. 2018;553(7689):446–454. doi:10.1038/nature25183
4. Paez JG, Jänne PA, Lee JC, et al. EGFR mutations in lung cancer: correlation with clinical response to gefitinib therapy. *Science*. 2004;304(5676):1497–1500. doi:10.1126/science.1099314
5. Wheeler DL, Dunn EF, Harari PM. Understanding resistance to EGFR inhibitors-impact on future treatment strategies. *Nat Rev Clin Oncol*. 2010;7(9):493–507. doi:10.1038/nrclinonc.2010.97
6. Cohen MH, Johnson JR, Chen Y-F, et al. FDA drug approval summary: erlotinib (Tarceva®) tablets. *Oncologist*. 2005;10(7):461–466. doi:10.1634/theoncologist.10-7-461
7. Benet LZ, Broccatelli F, Oprea TI. BDDCS applied to over 900 drugs. *AAPS J*. 2011;13(4):519–547. doi:10.1208/s12248-011-9290-9
8. Tóth G, Jánoska Á, Szabó Z-I, et al. Physicochemical characterisation and cyclodextrin complexation of erlotinib. *Supramol Chem*. 2016;28(7–8):656–664. doi:10.1080/10610278.2015.1117083
9. Truong DH, Tran TH, Ramasamy T, et al. Development of solid self-emulsifying formulation for improving the oral bioavailability of erlotinib. *AAPS Pharm Sci Tech*. 2016;17(2):466–473. doi:10.1208/s12249-015-0370-5
10. Budha NR, Frymoyer A, Smelick GS, et al. Drug absorption interactions between oral targeted anticancer agents and PPIs: is pH-dependent solubility the achilles heel of targeted therapy? *Clin Pharmacol Ther*. 2012;92(2):203–213. doi:10.1038/clpt.2012.73
11. Di Gion P, Kanefendt F, Lindauer A, et al. Clinical pharmacokinetics of tyrosine kinase inhibitors. *Clin Pharmacokinet*. 2011;50(9):551–603. doi:10.2165/11593320-000000000-00000
12. Herbrink M, Nuijen B, Schellens JHM, et al. Variability in bioavailability of small molecular tyrosine kinase inhibitors. *Cancer Treat Rev*. 2015;41(5):412–422. doi:10.1016/j.ctrv.2015.03.005
13. Lynch TJ, Kim ES, Eaby B, et al. Epidermal growth factor receptor inhibitor-associated cutaneous toxicities: an evolving paradigm in clinical management. *Oncologist*. 2007;12(5):610–621. doi:10.1634/theoncologist.12-5-610
14. Clapes V, Rousseau V, Despas F, et al. Adverse drug reactions involving protein kinase inhibitors: a French pharmacovigilance database study comparing safety in younger and older patients (≥75 years) with cancer. *Pharmaceut Med*. 2019;33(1):21–27. doi:10.1007/s40290-018-0259-1
15. Togashi Y, Masago K, Fujita S, et al. Differences in adverse events between 250 mg daily gefitinib and 150 mg daily erlotinib in Japanese patients with non-small cell lung cancer. *Lung Cancer*. 2011;74(1):98–102. doi:10.1016/j.lungcan.2011.01.022
16. Urata Y, Katakami N, Morita S, et al. Randomized Phase III study comparing gefitinib with erlotinib in patients with previously treated advanced lung adenocarcinoma: WJOG 5108L. *J Clin Oncol*. 2016;34(27):3248–3257. doi:10.1200/JCO.2015.63.4154
17. Shepherd FA, Rodrigues Pereira J, Ciuleanu T, et al. Erlotinib in previously treated non–small-cell lung cancer. *N Engl J Med*. 2005;353(2):123–132. doi:10.1056/NEJMoa050753
18. Truong DH, Le VKH, Pham TT, et al. Delivery of erlotinib for enhanced cancer treatment: an update review on particulate systems. *J Drug Deliv Sci Technol*. 2020;2020:55.
19. Marslin G, Sheeba CJ, Kalaichelvan VK, et al. Poly(D,L-lactic-co-glycolic acid) nanoencapsulation reduces erlotinib-induced subacute toxicity in rat. *J Biomed Nanotechnol*. 2009;5(5):464–471. doi:10.1166/jbn.2009.1075
20. Kim J, Ramasamy T, Choi JY, et al. PEGylated polypeptide lipid nanocapsules to enhance the anticancer efficacy of erlotinib in non-small cell lung cancer. *Colloids Surf B*. 2017;150:393–401. doi:10.1016/j.colsurfb.2016.11.002
21. Zhou X, He X, Shi K, et al. Injectable thermosensitive hydrogel containing erlotinib-loaded hollow mesoporous silica nanoparticles as a localized drug delivery system for NSCLC therapy. *Adv Sci*. 2020;7(23):2001442. doi:10.1002/advs.202001442
22. Xu Y, Hsu JC, Xu L, et al. Nanomedicine-based adjuvant therapy: a promising solution for lung cancer. *J Nanobiotechnology*. 2023;21(1):211. doi:10.1186/s12951-023-01958-4
23. Peer D, Karp JM, Hong S, et al. Nanocarriers as an emerging platform for cancer therapy. *Nat Nanotechnol*. 2007;2(12):751–760. doi:10.1038/nnano.2007.387
24. Li F, Mei H, Gao Y, et al. Co-delivery of oxygen and erlotinib by aptamer-modified liposomal complexes to reverse hypoxia-induced drug resistance in lung cancer. *Biomaterials*. 2017;145:56–71. doi:10.1016/j.biomaterials.2017.08.030

25. Zhou Z, Kennell C, Jafari M, et al. Sequential delivery of erlotinib and doxorubicin for enhanced triple negative Breast cancer treatment using polymeric nanoparticle. *Int J Pharm*. 2017;530(1–2):300–307. doi:10.1016/j.ijpharm.2017.07.085
26. Dora CP, Trotta F, Kushwah V, et al. Potential of erlotinib cyclodextrin nanosponge complex to enhance solubility, dissolution rate, in vitro cytotoxicity and oral bioavailability. *Carbohydr Polym*. 2016;137:339–349. doi:10.1016/j.carbpol.2015.10.080
27. Bhatia SN, Chen X, Dobrovolskaia MA, et al. Cancer nanomedicine. *Nat Rev Cancer*. 2022;22(10):550–556. doi:10.1038/s41568-022-00496-9
28. Grimaldi N, Andrade F, Segovia N, et al. Lipid-based nanovesicles for nanomedicine. *Chem Soc Rev*. 2016;45(23):6520–6545. doi:10.1039/c6cs00409a
29. Forgham H, Zhu J, Qiao R, et al. Star Polymer Nanomedicines─challenges and future perspectives. *ACS Appl Polym Mater*. 2022;4(10):6784–6796. doi:10.1021/acsapm.2c01291
30. George TA, Chen MM, Czosseck A, et al. Liposome-encapsulated anthraquinone improves efficacy and safety in triple negative breast cancer. *J Control Release*. 2022;342:31–43. doi:10.1016/j.jconrel.2021.12.001
31. Steffes VM, Murali MM, Park Y, et al. Distinct solubility and cytotoxicity regimes of paclitaxel-loaded cationic liposomes at low and high drug content revealed by kinetic phase behavior and cancer cell viability studies. *Biomaterials*. 2017;145:242–255. doi:10.1016/j.biomaterials.2017.08.026
32. Guimarães D, Cavaco-Paulo A, Nogueira E. Design of liposomes as drug delivery system for therapeutic applications. *Int J Pharm*. 2021;601:120571. doi:10.1016/j.ijpharm.2021.120571
33. Fumagalli G, Marucci C, Christodoulou MS, et al. Self-assembly drug conjugates for anticancer treatment. *Drug Discov Today*. 2016;21(8):1321–1329. doi:10.1016/j.drudis.2016.06.018
34. Liu C, Liu C, Bai Y, et al. Drug self-delivery systems: molecule design, construction strategy, and biological application. *Adv Healthcare Mater*. 2023;12(10):2202769. doi:10.1002/adhm.202202769
35. Iyer AK, Khaled G, Fang J, et al. Exploiting the enhanced permeability and retention effect for tumor targeting. *Drug Discov Today*. 2006;11(17–18):812–818. doi:10.1016/j.drudis.2006.07.005
36. Maiti S, Park N, Han JH, et al. Gemcitabine-coumarin-biotin conjugates: a target specific theranostic anticancer prodrug. *J Am Chem Soc*. 2013;135(11):4567–4572. doi:10.1021/ja401350x
37. Ren WX, Han J, Uhm S, et al. Recent development of biotin conjugation in biological imaging, sensing, and target delivery. *Chem Comm*. 2015;51(52):10403–10418. doi:10.1039/C5CC03075G
38. Cong M, Xu G, Yang S, et al. A self-assembling prodrug nanosystem to enhance metabolic stability and anticancer activity of gemcitabine. *Chin Chem Lett*. 2022;33(5):2481–2485. doi:10.1016/j.cclet.2021.11.083
39. Kasai H, Murakami T, Ikuta Y, et al. Creation of pure nanodrugs and their anticancer properties. *Angew Chem Int Ed*. 2012;51(41):10315–10318. doi:10.1002/anie.201204596
40. Zhong ZX, Li XZ, Liu JT, et al. Disulfide bond-based SN38 prodrug nanoassemblies with high drug loading and reduction-triggered drug release for pancreatic cancer therapy. *Int J Nanomedicine*. 2023;18:1281–1298. doi:10.2147/IJN.S404848
41. Chen H, Khemtong C, Yang X, et al. Nanonization strategies for poorly water-soluble drugs. *Drug Discov Today*. 2011;16:354–360. doi:10.1016/j.drudis.2010.02.009
42. Da Silva FLO, Marques MBF, Kato KC, et al. Nanonization techniques to overcome poor water-solubility with drugs. *Expert Opin Drug Discov*. 2020;15(7):853–864. doi:10.1080/17460441.2020.1750591
43. Bruinsmann FA, Buss JH, Souto GD, et al. Erlotinib-loaded poly(ε-caprolactone) nanocapsules improve in vitro cytotoxicity and anticlonogenic effects on human A549 lung cancer cells. *AAPS Pharm Sci Tech*. 2020;21(6):229. doi:10.1208/s12249-020-01723-y